Two bisindoles, indirubin and indol-3-ylmethylene-2-oxoindole, produced by the blocked mutant B-4 of *Chromobacterium violaceum* and implications for their biosynthetic pathways

Hiroyasu TAMURA[1,2], Masato SATO[1,2], Manabu HIGUMA[2], Yoshiko SAKAGUCHI[2], Yusuke SASAKI[2] and Tsutomu HOSHINO[1,2]*

(Received October 7 2020)

ABSTRACT

A bacterium species, *Chromobacterium violaceum* produces deep violet pigments, violacein **1** and deoxyviolacein **2**, as tryptophan metabolites. A blocked mutant, B-4, which is prepared with *N*-methyl-*N'*-nitrosoguanidine (NTG) mutagenic agent, generated two bisindole metabolites, indirubin **16** and (*Z*)-indol-3-ylmethylene- 2-oxoindole **17**, which are known to exhibit pharmacological activities. These structures were proposed based mainly on the detailed analyses of 2D NMR data in addition to the analyses of electronic and IR spectra. This is the first report to describe the production of **16** and **17** by *C. violaceum*. In addition, we propose the plausible biosynthetic pathway for **16** and **17** from tryptophan molecule.

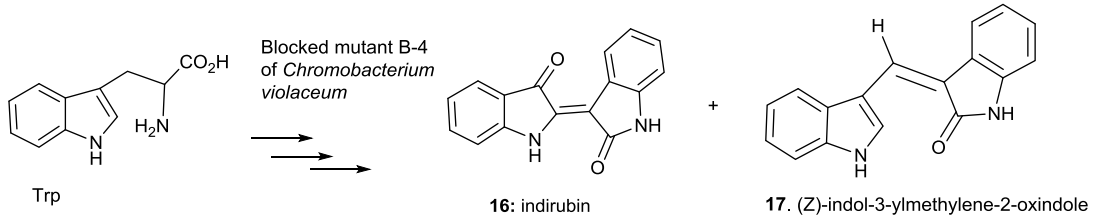

Bull.Facul.Agric.Niigata Univ., 73:1-11, 2021

Key words : violacein, bisindole, indirubin, (*Z*)-indol-3-ylmethylene-2-oxoindole, *Chromobacterium violaceum*.

Introduction

Violacein **1** and deoxyviolacein **2**, shown in Figure 1, are natural purple pigments produced by *Chromobacterium violaceum* (Review articles; Hoshino 2011, Ryan and Drennan 2009, Choi *et al*., 2015, Asamizu, 2017, Pauer *et al*., 2018, Rodrigues *et al*., 2013, de Carvalho *et al*., 2006, Bilsland *et al*., 2018). The bisindole pigments are reported to have interesting biological activities, such as antimicrobial, anticancer and antitrypanocidal activities (Choi *et al*., 2015, Pauer *et al*., 2018). The bisindole cores of **1** and **2** are closely related to those of rebeccamycin **3** (Nettleton *et al*., 1985, Bush *et al*., 1987) and staurosporin **4** (indolocarbazol skeleton) (Omura *et al*. 1977), which have potent inhibitory activities for kinase and topoisomerase-1, respectively (Choi *et al*., 2015). Since 1987, we have been disclosing biosynthetic studies on violacein. All the carbon, nitrogen and hydrogen atoms originate exclusively from two tryptophan (Trp) molecule (Hoshino *et al*., 1987a); the hydrogen atom of the 2-pyrrolidone moiety is derived from [side chain 3-H_S]Trp. The three oxygen atoms present in violacein **1** originate from molecular oxygen (Hoshino *et al*., 1987a, Hoshino and Ogasawara 1990). The most notable finding was that one of the two Trp molecules undergoes a 1,2-shift of the indole ring (Hoshino *et al*., 1987b), while the second one remains intact during biosynthesis, including its carboxyl group and nitrogen atom (Momen and Hoshino 2000); this finding has been elucidated by the feeding experiments of [side chain 3-^{13}C]Trp **20b** and [side chain 2-^{13}C]Trp **20c** (labeled with ■ and with ●, respectively, in Scheme 1). The 1,2-shift of indole ring has never been found in the biosynthetic processes of all the natural products so far; this is the first case.

We have succeeded in a molecular cloning of biosynthetic gene cluster of violacein (Figure 2). Five open reading frames (ORFs, VioA-E) are responsible for the biosynthesis of **1** (Shinoda *et al*., 2007), while four ORFs (VioA, B, C and E) participate in the biosynthesis of **2** (Hoshino, 2011, Sánchez *et al*., 2006, Balibar and Walsh, 2006). We have reported that a non-enzymatic oxidation process is involved in the construction of the violacein scaffold of **1** and **2** (Hoshino 2011, Shinoda *et al*, 2007), as shown in Scheme 1. VioA enzyme

[1] Graduate School of Science and Technology, Niigata University

[2] Faculty of Agriculture, Niigata University

* Corresponding author: hoshitsu@emeritus.niigata-u.ac.jp

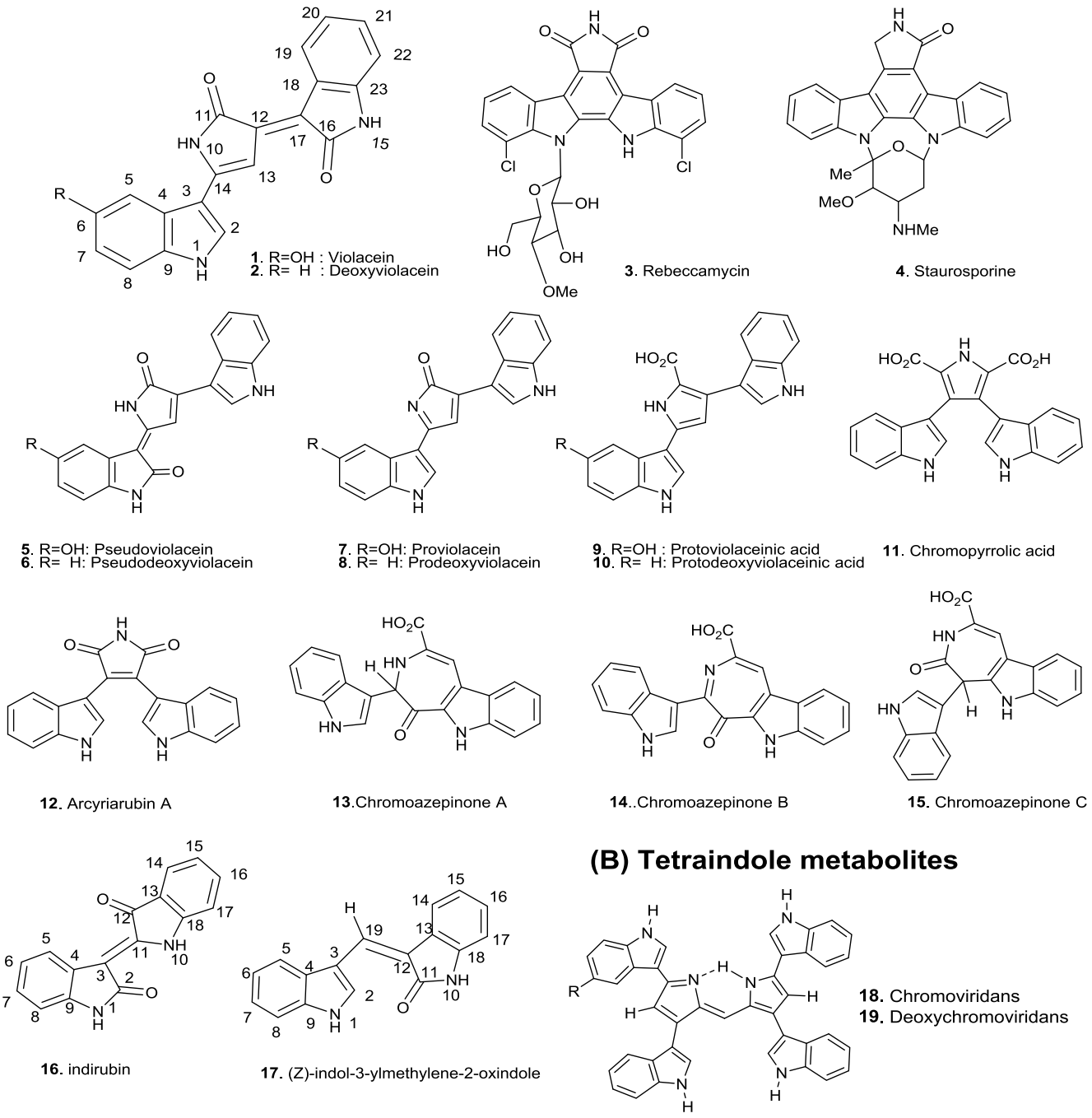

Figure 1. Tryptophan metabolites discussed in this paper. (A) and (B) indicate bisindole (**1** to **17**) and tetraindole compounds (**18** and **19**), respectively. All indole alkaloids **5** to **19** (new compounds) have been isolated in our biosynthetic studies.

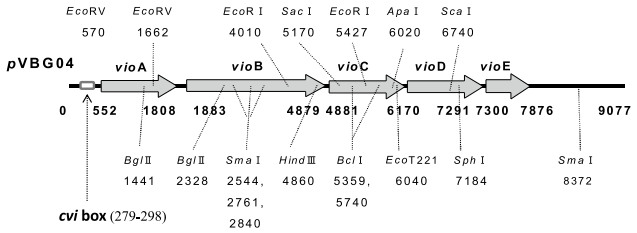

Figure 2. Restriction map of the biosynthetic gene cluster of violacein (accession number AB032799), which was cloned from *Chromobacterium violaceum* (JCM1249). The five genes (*vio*A-E) are transcribed in the same direction. The *cvi* box sequence (20-bp *lux* box-like palindromic sequence) in the *vio*A promoter region represents the binding site of CviR/AHL complex, regulating the expression of violacein biosynthetic gene cluster.

(L-Trp oxidase) containing a FAD cofactor (Shinoda *et al*., 2007, Füller *et al*., 2016) participates in the formation of indole pyruvic acid (IPA) imine **21** from Trp. VioB protein (heme-containing oxidase) catalyzes the coupling of two IPA imines to form the dimeric structure **22** (postulated due to the lability of this compound). As mentioned above, one of the two Trp molecules remains intact during the biosynthesis, (**20c** in Scheme 1, bonds represented in bold); both the nitrogen atom (bold) and the carboxyl group of **20c** are retained (Momen and Hoshino, 2000). The structures of ^{13}C-labeled Trps discussed here are shown in Scheme 1A. The nucleophilic amino group (bold) of **23** carries out an intramolecular attack onto the imino carbon to afford the pyrrole ring of **24**. Following the removal of an NH_3 to form **25**, an indole shift occurs according to the mechanism via a cyclopropane ring as shown in Scheme 1A, yielding protodeoxyviolaceinic acid **10**. These reactions are catalyzed by a newly-discovered enzyme, VioE protein (Sánchez *et al*., 2006, Balibar and Walsh, 2006, Ryan *et al*., 2008, Hirano *et al*., 2008). Although **10** is a labile molecule, the structure was successfully established by our NMR analyses (Shinoda *et al*., 2007). Protoviolaceinic acid **9**, which possesses a 5-hydroxy group on the north indole ring, is generated by FAD-containing VioD (Hoshino, 2011, Ryan *et al*., 2009, Asamizu, 2017, Shinoda *et al*., 2007, Sánchez *et al*., 2006, Balibar and Walsh, 2006). C-16 of **9** and **10** were then oxidized by the action of VioC protein to yield **26** and **27**, respectively. Intermediates **26** and **27** were further oxidized in the presence of molecular oxygen (1,4-addition of O_2) to afford **28**; the oxidative decarboxylation reaction of **28** occurs non-enzymatically, as shown in Scheme 1A (Shinoda *et al*., 2007). Consequently, violacein is biosynthesized via two processes: (1) the enzymatic processes of five enzymes VioA → VioB → VioE → VioD → VioC, and (2) a subsequent non-enzymatic oxygenation cascade. We have discovered metabolites **7** and **8**, the structures of which are very similar to those of **1** and **2**, respectively, implying that the oxygenation at C-16 of **7** and **8** may lead to the production of

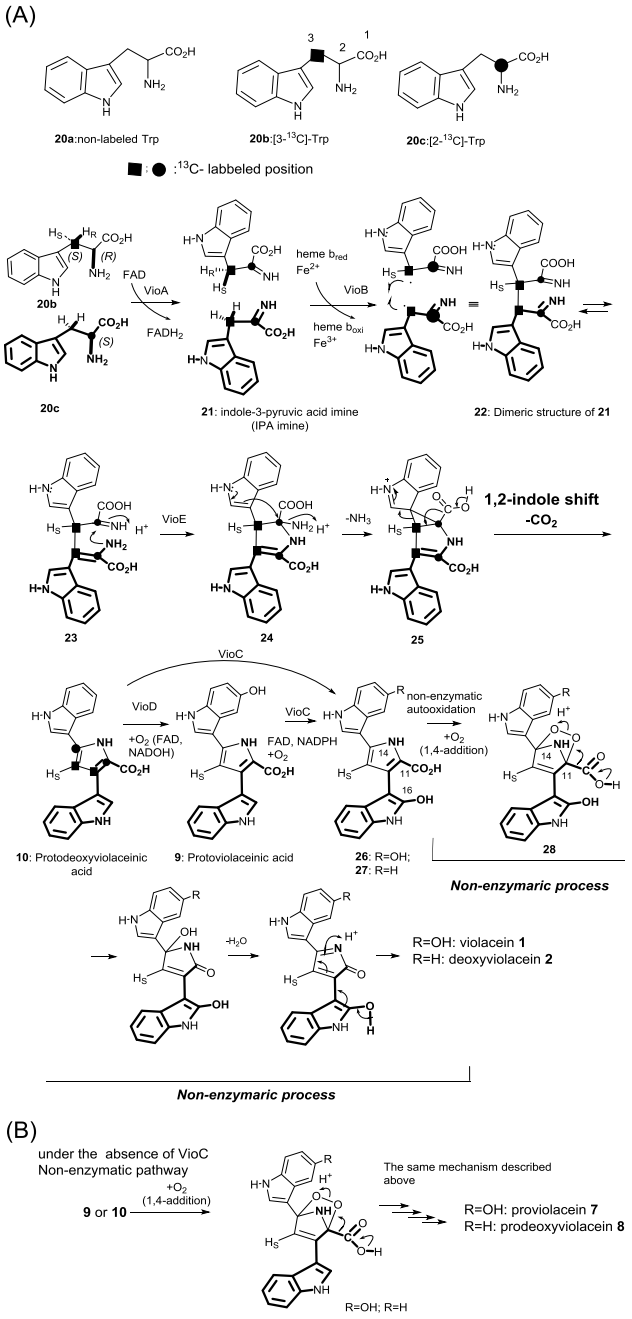

Scheme 1. (A) Biosynthetic pathway of violacein **1** and its deoxyhomolog **2** from Trp **20**. In addition to 5 open-reading frames VioA~E, non-enzymatic auto-oxidation processes of **9** and **10** (1,4-addition of molecular oxygen) are involved in the biosynthetic pathway. (B) Production mechanism of proviolacein **7** and prodeoxyviolacein **8** from **9** and **10**, respectively, where all the process proceeds under non-enzymatic auto-oxidation.

1 and **2**; however, **7** and **8** were not transformed into **1** and **2** by the washed whole cells of the parent strain (Momen *et al*., 1998). This finding demonstrates that **7** and **8** are not genuine biosynthetic intermediates. Therefore, **7** and **8** were produced non-enzymatically from **9** and **10**, respectively, by the oxidative decarboxylation mechanism shown in Scheme 1B (Hoshino, 2011, Shinoda *et al*., 2007).

Figure 1 depicts the tryptophan metabolites (**5**–**19**) that we have discovered through our biosynthetic investigations on violaceins **1** and **2**. Bisindole metabolites **5**–**8** were produced by the addition of diethyldithiocarbamate to the washed whole cells of *C. violaceum* (Hoshino *et al*.,1994, Hoshino *et al*. 1997), under the same conditions that result in the production of **1** and **2** from Trp. Protoviolaceinic acids **9** and **10** were isolated following the incubation of Trp for a short period with the cell-free extracts consisting of four enzymes, VioA, B, D, and E, and three enzymes, VioA, B and E, respectively, in the presence of NADPH (Shinoda *et al*., 2007, Hoshino and Yamamoto, 1997). In addition to genetic studies, we have prepared blocked mutants by employing the mutagenic agent *N*-methyl-*N'*-nitrosoguanidine (NTG), in order to investigate the biosynthetic mechanism in more detail. Several blocked mutants prepared in this manner generated novel bisindole metabolites **11** (Hoshino *et al*., 1993), **12**–**15** (Mizuoka *et al*., 2010), and tetraindole pigments **18** and **19** (Momen *et al*., 1998). The discovery of these novel bis- and tetra-indole compounds impelled us to prepare additional blocked mutants. This study reports the structure determination of bisindoles **16** (indirubin, red color) and **17** (indol-3-ylmethylene-2-oxindole, yellow) obtained from a B-4 mutant, the bisindole scaffolds **16** and **17** by *C. violaceum* having not been reported hitherto. Furthermore, we discuss the production pathways of **16** and **17** from Trp **20a**.

Materials and Methods

Instruments

UV spectra were measured on a JASCO Ubest-30 spectrophotometer. IR spectra with a JASCO IR-700 spectrophotometer. NMR spectra of **16** were recorded in DMO-d_6 on a Bruker DPX 400 spectrometer, the chemical shifts being relative to the solvent peak δ_H 2.49 and δ_C 39.50 as the internal reference for ^{1}H and ^{13}C NMR spectra, respectively. NMR spectra of **17** diacetate were measured in $CDCl_3$; the residual solvent peak was adjusted at 7.26 ppm for the ^{1}H NMR and 77.0 ppm for ^{13}C NMR. MS spectra of (EI, CI and FABMS) were obtained with a JEOL SX 100 mass spectrometer (isobutane gas for CIMS).

Isolation of metabolites 16 and 17 from the blocked mutant B-4.

Production amounts of **16** and **17** were higher in a solution of pH 7.2 than those in a solution of pH 8.5. Thus, we incubated in a phosphate buffer pH 7.2. The culture medium and incubation conditions of B-4 strain were the same as that of our previous reports (Hoshino *et al*., 1995, Hoshino and Yamamoto 1997, Hoshino *et al*., 1993, Mizuoka *et al*., 2010).The washed whole cells from 1L culture were suspended in a solution containing 5 mg of Trp in a pH 7.2 phosphate buffer (5 mL) and incubated at 25 ℃ for 48 h on a rotary shaker (180 rpm). The isolations were conducted according to the protocol described in the Results and Discussion section. The yields of **16** and **17** from 50 mg of Trp were ca 2 mg and 5 mg, respectively.

Spectroscopic data of products 16 and 17.

Product ***16****: indirubin,* (*Z*)-[2,3'-biindolinylidene]-2',3-dione. Red powder. M.p. > 300 ℃. UV-visible spectrum in MeOH; $\lambda_{max}(\varepsilon)$ 536 nm (4800), 360 nm (3060); 287.5 nm (12800). IR spectrum (KBr): 1660 and 1620 cm^{-1}, which were suggestive of the presence of conjugated carbonyl group and/or amide functional group. HREIMS *m/z* 262.0761(calcd for $C_{16}H_{10}O_2N_2$, 262.0742). ^{1}H NMR (400 MHz) in DMSO-d_6; δ_H (ppm) 11.01 (H-1, br s, 1H), 10.89 (H-10, br s, 1H), 8.75 (H-14, d, *J*=7.6 Hz, 1H), 7.65 (H-5, d, *J*=7.6 Hz, 1H), 7.57 (H-7, dt, *J*=7.6, 1.2 Hz, 1H), 7.41 (H-8, d, *J*=7.8 Hz,1H), 7.24 (H-16, br t, *J*=7.6, 0.8 Hz), 7.01 (H-15, t, *J*=7.8 Hz,1H), 7.01 (H-6, t, *J*=7.6 Hz, 1H), 6.83 (H-17, d, *J*=7.6 Hz); ^{13}C NMR (100 MHz) in DMSO d_6, δ_C (ppm) 106.6 (C-13, s), 109.6 (C-17, d), 113.5 (C-8, d), 119.0 (C-4, s), 121.3 (C-6 and C-15, d), 121.5 (C-11, s), 124.4 (C-5, d), 124.7 (C-14, d), 129.3 (C-16, d), 137.2 (C-7, d), 138.4 (C-3, s), 140.9 (C-18, s), 152.5 (C-9, s), 171.0 (C-12, s), 188.7 (C-2, s); see also Table 1.

Product ***17****: (Z)-3-((1H-indol-3-yl)methylene)indolin-2-one.*

Yellow powder. M.p. > 220 ℃. UV-visible spectrum in MeOH is shown in Figure SIV-1; $\lambda_{max}(\varepsilon)$ 405.5 nm (17600), 263.5 nm (12500). IR spectrum: 1660 and 1620 cm^{-1}, which is indicative of the presence of conjugated carbonyl group and/or amide functional group. EIMS of **17** showed a prominent peak at *m/z* 260 (M^+) and its diacetate of **17**, prepared with Ac_2O/Py, exhibited *m/z* 344 (M^++2×Ac). HREIMS of **17** *m/z* 260.0980 (calcd for $C_{17}H_{12}ON_2$, 260.0950). 1D- and 2D-NMR spectra of the diacetate of **17** was measured in $CDCl_3$: ^{1}H NMR (400 MHz) of the diacetate in $CDCl_3$: δ_H (ppm) 2.79 (Ac-CH_3, s, 3H), 2.81 (Ac-CH_3, s, 3H), 7.24 (H-15, br t, *J*=8.0 Hz), 7.35 (H-16, bt, *J*=8.0 Hz), 7.44 (H-6 and H-7, m, 2H), 7.67 (H-14, d, *J*=8.0 Hz, 1H), 7.82 (H-5, m, 1H), 7.85 (H-19, s, 1H), 8.28 (H-17, d, *J*=8.0 Hz), 8.53 (H-8, m, 1H), 9.56 (H-2, s, 1H); ^{13}C NMR (100 MHz) in $CDCl_3$, δ_C (ppm) 24.09 (Ac-*C*H$_3$, q), 26.98 (Ac-*C*H$_3$, q), 115.7 (C-3, s), 116.6 (C-17, d), 117.7 (C-5, d), 118.1 (C-14, d), 122.9 (C-12, s), 124.5 (C-6, d), 124.7 (C-8 and C-15, d), 125.7 (C-19, d), 126.1 (C-7, d), 129.18 (C-16, d), 130.1 (C-4, s), 130.2 (C-13, s), 132.2 (C-2, s), 135.4 (C-9, s), 138.1 (C-18, s), 167.0 (C-11, s), 169.3 (Ac-*C*O, s), 171.1 (Ac-*C*O, s), the assignments of C-4 and C-13 may be exchangeable; see also Table 2.

Results and Discussion

Isolation of 16 and 17

Tryptophan metabolites **16** and **17** were extracellular metabolites produced by the mutant B-4. The supernatant obtained following centrifugation was dried and MeOH was

added to the residues in order to extract crude **16** and **17**, which were then dried and dissolved in EtOAc. Subsequently, the EtOAc solution containing crude **16** and **17** was fractionated into three components: acidic, neutral and basic compounds. Metabolites **16** and **17** remained in the neutral fraction. Pure **16** and **17** were obtained by column chromatography with a SiO_2 eluting with 100% $CHCl_3$, followed by chromatography on a Sephadex LH 20 column, eluting with MeOH.

Structures of 16 and 17 produced by mutant B-4

Tryptophan metabolites **16** and **17** were isolated from the blocked mutant B-4.

Metabolite **16** was red in color: λ_{max} 536 nm in MeOH. EIMS and CIMS indicated *m/z* 262 and *m/z* 263 as prominent ions, respectively, implying that the molecular weight of **16** is 262, and HR-EIMS analysis provided the molecular formula $C_{16}H_{10}O_2N_2$. The ^{1}H-^{1}H COSY and NOESY spectra in DMSO-d_6 indicated the presence of two indole rings (see Figure 3); however, H-2 of the two indole rings was missing (absence of NOE and COSY cross peaks between N*H* and H-2). Instead, two carbonyl carbons (δ_C 188.7, s; δ_C 171.0, s) were found in the ^{13}C NMR (Table 1). The two carbonyl signals exhibited distinct HMBC correlations with N*H* protons (H-1 and H-10) of the indole rings (see Figure 3). In addition to the two phenyl carbons (12×C) in the indole rings and two carbonyl carbons (2×C), signals for two tetrasubstituted sp^2 carbons (2×C) were detected at δ_C 138.4 (s) and 121.5 (s) (see Table 1). The total numbers of carbon, hydrogen and nitrogen atoms obtained from the NMR spectra fulfill the molecular formula $C_{16}H_{10}O_2N_2$. In general, HMBC cross peaks are found between ^{1}H and ^{13}C that are separated with both two- and three bonds. Therefore, we can suppose that **16** is composed of 2- and/or 3-oxindoles, which are connected at C2-C2, C2-C3 or C3-C3 of the two oxindole rings through a double bond, as shown in Figure 3B, 3A and 3C, respectively. Thus, three isomers (indirubin, isoindigo and indigo) can be proposed (see Figure 3A, B and C).

The production of indigo by *C. violaceum* has been reported by Cheah *et al* (Cheah *et al.* 1998). Indirubin **16** is constructed by both 2- and 3-oxindoles, which are connected through the double bond at C-3 and C-2 of the oxindole nuclei. Isoindigo **29** consists of both 2- and 2-oxindoles that are connected at C-3 and C-3 of the 2-oxindole rings. Indigo **30** is assembled from both 3- and 3-oxindoles, which are bonded at C-2 and C-2 of the oxindole cores. Isomers **16**, **29** and **31** all exist as both (*E*)- and (*Z*)-isomers (see the structures in Figure 3, Maugard T. *et al.* 2001). Both **29** and **30** have a plane of symmetry in their structures and further have C2 rotation axis (shown by bold and curved lines), thus the number of carbons and protons in the NMR spectra amount to half of that in their molecular formula. However, the ^{1}H and ^{13}C NMR spectra of **16** contained signals for 10 protons and 16 carbons, the same number as that of the molecular formula, suggesting that **16** is indirubin, as shown in Figure 3A, but not isoindigo **29** and indigo **30**. We could not assign (*E*) or (*Z*)-configurations for **16** based on NOESY data alone, as no NOEs were found between the protons of the two oxindole rings. Detailed analyses of NOESY and HMBC spectra are shown in Figure 3. UV-visible spectra of **16**, **31** and **32** have been reported (Maugard *et al.*, 2001). Pigments **16**, **29** and **30** were reported as being red, brown and blue in color, respectively. As described above, isolated **16** was red in color. The absorption spectrum of **16** was analogous to that reported by Maugard *et al.*, and Ju *et al.*, (Maugard *et al.*, 2001, Ju *et al.*, 2019). Thus, structure of isolated **16** was determined to be either (*E*)- or (*Z*)-indirubin. The NMR data are tabulated in Table 1. Furthermore, Maugard *et al.* reported that the UV-visible spectra of the (*E*)-isomers of **16**, **29** and **30** are identical to those of the corresponding (*Z*)-isomers (Maugard *et al.*, 2001). It is known that indirubin and its analogs can be used to treat various diseases, including granulocytic leukemia, cancer, and Alzheimer's disease (Du et al., 2018, Fiebig and Schüler, 2006).

Metabolite **17** appeared yellow in color (λ_{max} 405.5 nm). The spectrum was not altered by the addition of trace amounts of TFA (trifluoroacetic acid) or NH_3, indicating the absence of basic and acidic functional groups. The EIMS spectrum of **17** indicated *m/z* 260 as the heaviest ion; the acetate derivative, prepared by Ac_2O/Py, presented *m/z* 344 as the prominent ion ($M^+ + 2\times Ac$). Hence, a diacetate of **17** was produced, which further indicated that the M^+ of isolated

Table 1. Completely assigned chemical shifts of ^{1}H- and ^{13}C signals for **16**, which were measured in DMSO d_6.

Positions	^{1}H: δ_H (ppm), *J* (Hz)	^{13}C: δ_C (ppm)
1	11.01 (bs, 1H)	—
2	—	188.7 (s)
3	— —	138.4 (s)
4	—	119.0 (s)
5	7.65 (d, 7.6 Hz, 1H)	124.4 (d)
6	7.01 (t, 7.6 Hz, 1H)	121.3 (d)
7	7.57 (t-like, 7.6, 1.2 Hz, 1H)	137.2 (d)
8	7.41 (d, 7.8 Hz, 1H)	113.5 (d)
9	—	152.5 (s)
10	10.89 (bs, 1H)	—
11	—	121.5 (s)
12	—	171.0 (s)
13	—	106.6 (s)
14	8.75 (d, 7.6 Hz, 1H)	124.7 (d)
15	7.01 (t, 7.8 Hz, 1H)	121.3 (d)
16	7.24 (bt, 7.6, 0.8 Hz, 1H)	129.3 (d)
17	6.83 (d, 7.6 Hz, 1H)	109.6 (d)
18	—	140.9 (s)

The ^{1}H and ^{13}C-NMR data at 6- and 15-positions were identical.
Multiplicity in ^{1}H-NMR; s: singlet, d: doublet, t: triplet.
Multiplicity in ^{13}C-NMR inferred by DEPT spectra;
s: quaternary carbon; d: CH (methine carbon).

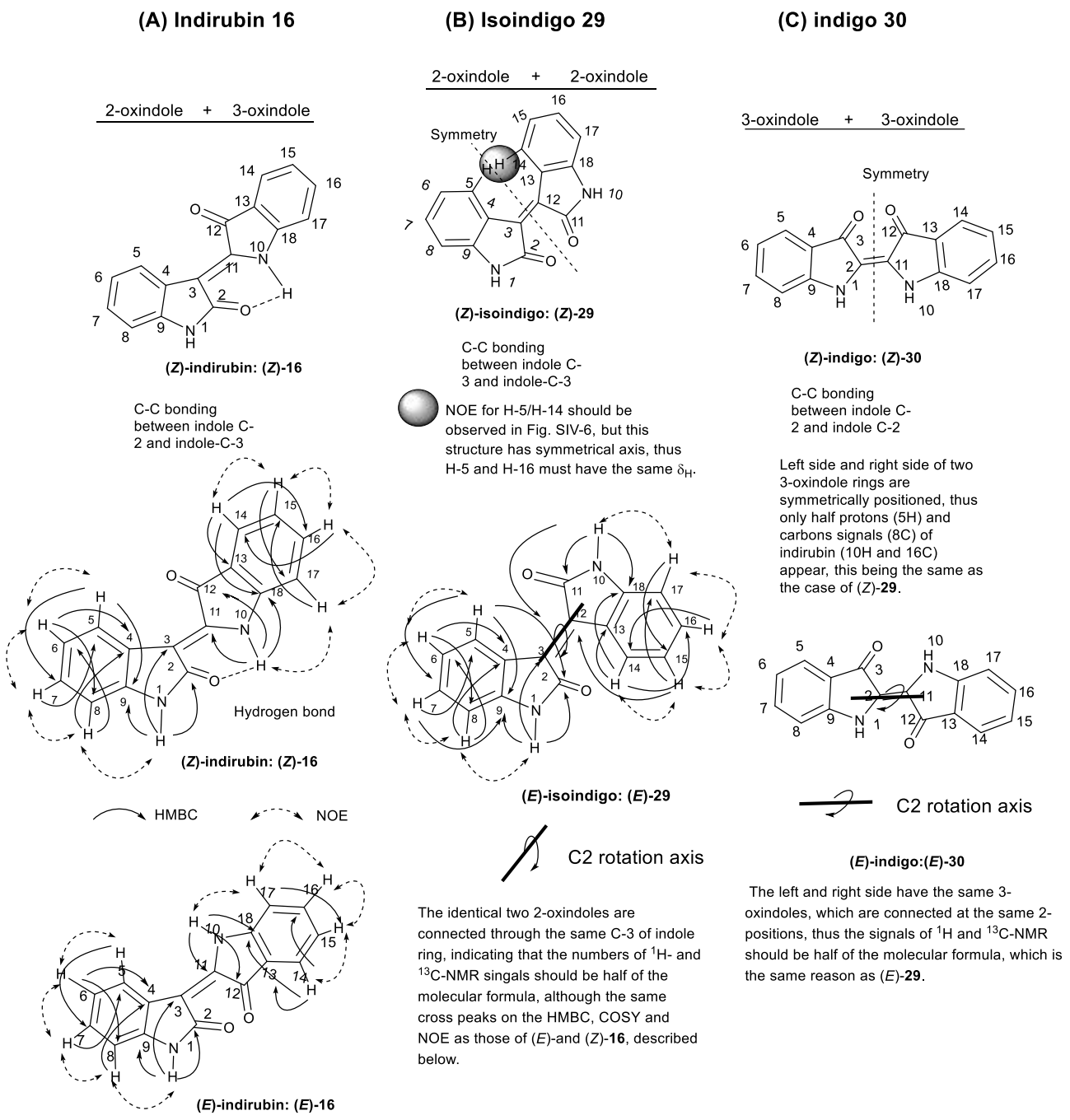

Figure 3. Three isomers (indirubin, isoindigo and indigo) proposed for the structure of red pigment **16**. Two oxindole rings are bonded through C-2/C-3 (indirubin), through C-2/C-2 (isoindigo) and through C-3/C-3 (indigo). (*Z*)-Isoindigo **29** and (*Z*)-indigo **30** both have a symmetrical planes (dotted line), thus the numbers of ^{13}C and ^{1}H signals must be half (C_8H_{15}) of the molecular formula ($C_{16}H_{10}O_2N_2$). In addition, those of the *E*-forms of **29** and **30** also become half of that in the molecular formula, because C2 rotation axises exist as shown by bold line and curved line (Figure 3). This figure also shows the NOEs and HMBC correlations found in the 2D NMR spectra of (*Z*)-**16**. (*E*)-**16** is also possible, but the (*Z*)-geometry is more favored than the *E*-form, because the hydrogen bonding is constructed for the *Z*-structure.

17 is 260. The molecular formula of **17** was determined to be $C_{17}H_{12}ON_2$ by HR-EIMS. Two acetate Me groups (6×H) were found at δ_H 2.79 (s) and 2.31 (s) in the ^{1}H NMR spectrum (400 MHz, $CDCl_3$); in the ^{13}C NMR (100 MHz), signals at δ_C 24.09 (q) and 26.98 (q) were assigned to the acetyl Me carbons, and δ_C 169.3 (s) and 171.1 (s) to the acetyl carbonyl carbons (*C*O) by its HMBC spectrum (see Figure 4). The NOE and COSY data of the diacetate confirmed the presence of two indole ring protons, as shown in Figure 4. However, only one proton at the C-2 position of the indole ring (H-2, δ_H 9.56, s, 1H) was observed, despite two indole rings being involved, suggesting that the H-2 of the second indole ring is substituted. The molecular formula indicated that **17** contains one oxygen atom, thus the second indole ring is suggested to be a 2-oxindole, which was further supported by the presence of a signal at δ_C 167.0 (s) in the ^{13}C NMR. This carbonyl carbon had a distinct HMBC correlation with one hydrogen atom (H-19, δ_H 7.85, s, 1H, olefinic proton), which is not present in the indole and oxindole rings. The δ_C of C-19 was 125.7 (d), as determined by the HMQC analysis. H-19 exhibited a clear HMBC correlation with C-2 and typical allylic spin-spin coupling $^4J_{H2\text{-}H19}$ (Figure 4). In addition, a clear NOE was observed between H-14 and H-19 (Figure 4), confirming that this double bond had a (*Z*)-configuration. Consequently, yellow metabolite **17** was determined to be (*Z*)-indol-3-ylmethylene-2-oxindole, and the structure is shown in Figure 1 and Figure 4. The NMR data are shown in the Table 2. Pharmacological activities of **17** and its derivatives have been reported, and include TPK receptor antagonist activity and applicability as agents against multiple sclerosis (Timmusk *et al*., 2017; Duvold *et al*., 2006).

Putative biosynthetic pathways for 16 and 17

Scheme 2A illustrates the proposed pathway of Trp to **16**. However, these propositions are tentative, as the experimental evidence using the B-4 mutant are lacking. The biosynthetic pathway for **16** by microorganisms (Qu *et al*., 2012) and plants (Maugard *et al*., 2001) has been reported. The tryptophanase enzyme converts Trp into indole **31**, pyruvic acid and ammonia. Next, **31** is oxidized to yield indoxyl **32**, which is further oxidized to afford isatin **33**. Condensation of **32** and **33** afforded **16**. INDO, a redox flavo-enzyme that converts **31** into **32**, was identified from *Chromobacterium violaceum* (Cheah *et al*., 1998). Air oxidation transforms **32** into indigo **30**. Decomposition of **30** affords **33** (Qu *et al*., 2012).

Schemes 2B and 2C suggest the production pathway for **17** from mutant B-4. Scheme 2B shows the condensation reaction of indole caboxaldehyde **34** with **31**, yielding **35**. Intermediate **34** is reportedly generated from tryptophan metabolism by *C. violaceum* (DeMoss, 1957). A subsequent dehydration reaction yields **36**, bearing a methenyl group (-CH=). Then, **36** likely gets oxygenated by VioC (see Scheme 1 and Figure 2) containing the Rossmann fold FAD (GxGxxG sequence motif; Shinoda *et al*., 2007; Qu *et al*., 2012), affording **37**, which is converted into the final product **17**, as shown in

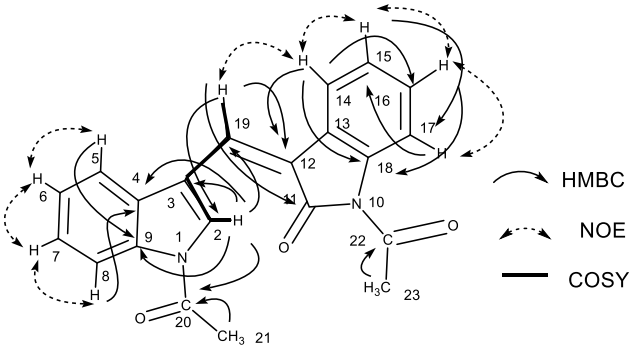

Figure 4. Key correlations of ^{1}H-^{1}H COSY, NOE and HMBC correlations of diaceylated **17**: (*Z*)-indol-3-ylmethylene-2-oxindole diacetate.

Table 2. ^{1}H- and ^{13}C NMR data of diacetylated **17** measured in $CDCl_3$.

Positions	^{1}H: δ_H (ppm), *J* (Hz)	^{13}C: δ_C (ppm)
1	—	—
2	9.56 (s, 1H)	132.2 (d)
3	—	115.7 (s)
4	—	130.1 (s)
5	7.82 (m, 1H)	117.7 (d)
6	7.44 (m, 1H)	124.5 (d)
7	7.44 (m, 1H)	126.1 (d)
8	8.53 (m, 1H)	124.7 (d)
9	—	135.4 (s)
10	—	—
11	—	167.0 (s)
12	—	122.9 (s)
13	—	130.s (s)
14	7.67 (d, 8.0 Hz, 1H)	118.1 (d)
15	7.24 (bt, 8.0 Hz, 1H)	124.7 (d)
16	7.35 (bt, 8.0 Hz, 1H)	129.2 (d)
17	8.28 (d, 8.0 Hz, 1H)	116.6 (d)
18	—	138.1 (s)
19	7.85 (s, 1H)	125.7 (d)
20	—	169.3 (s)
21	2.31 (s, 3H)	24.09 (q)
22	—	171.1 (s)
23	2.79 (s, 3H)	26.98 (q)

The δ_H at 6-, 7-positions were identical. The δ_C at 4- and 13-positions are exchangeable.

Multiplicity in ^{1}H-NMR; s: singlet, d: doublet, t: triplet, m: multiplet.

Multiplicity in ^{13}C-NMR inferred by DEPT spectra; s: quaternary carbon; d: CH (methine carbon), q: CH_3

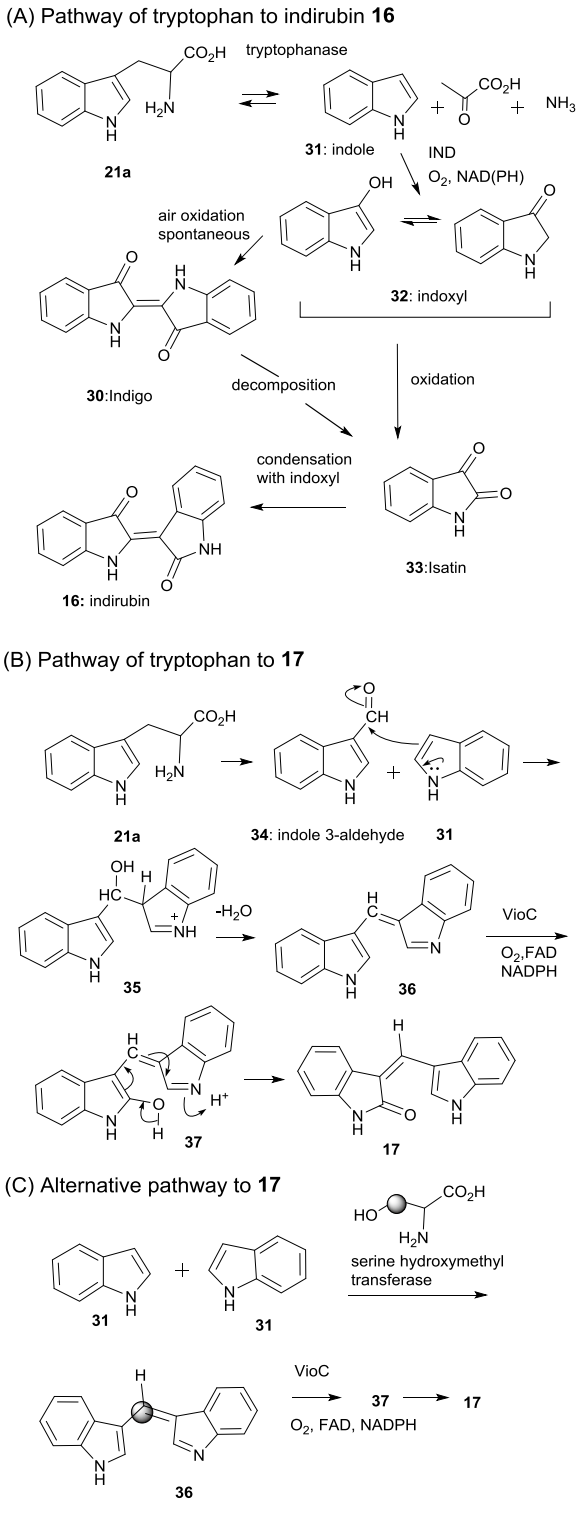

Scheme 2. Tentatively proposed biosynthetic pathways to **16** and **17** from tryptophan.
(A) Production pathway for **16**.
(B) Production mechanism for **17** via indole carboxaldehyde.
(C) Alternative biosynthetic pathway for the production of **17** via serine hydroxymethyl transferase (C_1 unit carrier).

Scheme 2B. Alternatively, the methenyl moiety may be derived from the C_1 unit of serine, via a reaction possibly catalyzed by serine hydroxymethyl transferase; we have reported definitive experimental evidence that this methenyl C_1 unit was also incorporated in the biosyntheses of tetraindole pigments chromoviridans **18** and deoxychromoviridans **19** (see Figure 1, Momen *et al*., 1998). Schemes 2B and 2C are therefore tentative at the current stage. No reports could be found regarding the biosynthetic pathway for **17** and its related compounds, although there are numerous reports concerning their chemical syntheses and bioactivities (ACS SciFinder). Further experiments are therefore necessary for a credible proposal on the biosynthetic pathways for **16** and **17** in *C. violaceum*, based on experimental observations.

Conclusions

Herein, we disclosed that B-4 mutant produced indirubin **16** and (*Z*)-3-((1*H*-indol-3-yl)methylene)indolin-2-one **17**, which are known compounds; however, the production of these two bisindole compounds by *C. violaceum* has not been reported hitherto. As shown in Figure 1, we have isolated a variety of tryptophan metabolites **5**–**19** from our biosynthetic studies of violacein by using enzyme inhibitors and NTG-treated mutants, in conjunction with genetic studies employing all of the VioA–E enzymes. At the present time, the production pathways of **16** and **17** have not been established, but we can propose the plausible biosynthetic pathways for the conversion of Trp into **16** and **17** based on the pathways proposed by other workers. B-4 variant never furnished violacein **1** and deoxyviolacein **2**, but the bisindole compounds were generated; this would suggest that the four genes *vio A, B, E* and *D* had been disrupted, but *vio* C still worked. In conclusion, we have demonstrated that treatments of the mutagenic agents toward the *whole cells* of microorganisms are also useful for further generating previously unknown and known compounds in future, as well as the mutations and the depletions of each of ORFs, through the biosynthetic studies on purplish blue pigment of violacein **1**.

References

Asamizu S. 2017. Biosynthesis of nitrogen-containing natural products, C_7N aminocyclitols and bis-indoles, from actinomycetes, *Biosci. Biotechnol. Biochem*. **81**: 871-881 (Review).

Balibar, C.J. and C.T.Walsh, 2006. In vitro biosynthesis of violacein from L-tryptophan by the enzymes VioA-E from *Chromobacterium violaceum*. *Biochemistry*, **45**: 15444-15457.

Bilsland, E., T.A. Travella, R. Krogh, J.E. Stokes, A. Roberts, J. Ajioka, D.R. Spring, A.D. Andricopulo, F.T.M. Costa and S.G. Oliver, 2018. Antiplasmodial and trypanocidal activity of violacein and deoxyviolacein produced from synthetic operons. *BMC Biotechnol*. **18**: 22 (Review).

Bush, A., B.H. Long, J.J. Catino, W.T. Bradner and K. Tomita,

1987. Production and biological activity of rebeccamycin, a novel antitumor agent. *J. Antibiot.* (Tokyo), **40**: 668-678.

Cheah, E., K. MacPherson, D. Quiggin, P. Keese and D.L. Ollis, 1998. Crystallization and preliminary X-ray analysis of IND, an enzyme with indole oxygenase activity from *Chromobacterium violaceum*. *Acta Cryst*, D54, 657-658.

Choi, S.Y., K.H. Yoon, J.I. Lee, R.J.Mitchell, 2015. Violacein: properties and production of a versatile bacterial pigment. *Biomed Res. Int.*, Article ID: 4605056 (Review).

de Carvalho D.D., F.T.M. Costa, N. Duran, M. Haun, 2006. Cytotoxic activity of violacein in human colon cancer cells, *Toxicol in Vitro,* **20**: 1514-1521 (Review).

DeMoss R.D and N.R. Evans, 1957. L-Tryptophan metabolism in *Chromobacterium violaceum., Bacterial Proc.*, 117.

Du J., D. Yang, Z.W. Luo and S.Y Lee, 2018, Metabolic engineering of *Escherichia coli* for the production of indirubin from glucose. *J. Biotechnol.*, **267**: 19-28.

Duvold L.M.E., S.E. Havez, E.T. Binderup and G.K. Andersem, 2006. Preparation of indolinone derivatives for treatment of multiple sclerosis. *PCT Int. Appl.*, WO 2006105796 A1 20061012.

Fiebig H-H. and J.B. Schüler, 2006. Chapter 21, *In vivo* antitumor activity of 5-methyl-indirubin. In *Indirubin, the Red Shade of Indigo*, ed. L. Meijer, L. S. Guyard, and G. Eisenbrand, D2D Book, Berkshire.

Füller J.J., R. Röpke, J. Krausze, K.E. Rennhack, N.P. Daniel, W. Blankenfeldt S. Schulz, D. Jahn and J. Moser, 2016. Biosynthesis of violacein, structure and function of L-tryptophan oxidase VioA from *Chromobacterium violaceum*. *J. Biol. Chem.*, **291**: 20068-20084.

Hirano, S., S. Asamizu, H. Onaka, Y. Shiro and S. Nagano, *J. Biol. Chem.*, 2008. Crystal structure of VioE, a key player in the construction of the molecular skeleton of violacein. **283**: 6459-6466.

Hoshino T., T. Takano, S. Hori and N. Ogasawara, 1987a. Biosynthesis of violacein: Origins of hydrogen, Nitrogen and Oxygen atoms in the 2-pyrrolidone nucleus. *Agric. Biol. Chem.* **51**: 2733-2741.

Hoshino T., T. Kondo, T. Uchiyama and N. Ogasawara, 1987b. Biosynthesis of violacein: a Novel rearrangement in tryptophan metabolism with a 1,2-shift of the indole ring. *Agric. Biol. Chem.***51**: 965-968.

Hoshino T. and N. Ogasawara, 1990. Biosynthesis of violacein: *Agric. Biol. Chem.* **54**: 2339-2746.

Hoshino T., Y. Kojima, T. Hayashi, T. Uchiyama and T. Kaneko, 1993. A new metabolite of tryptophan, chromopyrrolic acid, produced by *Chromobacterium violaceum, Biosci. Biotechnol. Biochem.,* **57**: 775-781.

Hoshino T., T. Hayashi and T. Uchiyama, 1994. Pseudodeoxyviolaceion, a new red pigment produced by the tryptophan metabolism of *Chromobacterium violaceum*, *Biosci. Biotechnol. Biopchem.*, **58**: 279-282.

Hoshino T., T. Hayashi and T. Odajima, 1995. Biosynthsis of violacein: oxygenation at the 2-pyrrolidone of the indole ring and structures of proviolacein, prodeoxyviolacein and pseudoviolacein, the plausible biosynthetic intermediates of violacein. *J. Chem. Soc., Perkin Trans. I,* 1565-1571.

Hoshino T. and M. Yamamoto, 1997. Conversion from tryptophan precursor into violacein pigments by a cell-free system from *Chromobacterium violaceum*, *Biosci. Biotechnol. Biochem.,* **61**: 2134-2136.

Hoshino T. 2011. Violacein and related tryptophan metabolites produced by *Chromobacterium violaceum*: biosynthetic mechanism and pathway for construction of violacein core. *Appl. Microbiol. Biotechnol.* **91**: 1463-1475 (Review).

Ju Z., J. Sun and Y. Liu, 2019. Molecular structures and spectral properties of natural indigo and indirubin: experimental and DFT studies. *Molecules* **24**: 3831.

Maugard T., E. Enaud, P. Choisy and M.D. Legoy, 2001. Identification of an indigo precursor from leaves of *Isatis tinctoria* (Woad). *Phytochemistry*, **58**: 897-904.

Mizuoka T., K. Toume and M. Ishibashi and T. Hoshino, 2010. Novel tryptophan metabolites, chromoazepinone A, B and C, produced by a blocked mutant of *Chromobacterium violaceum*, the biosynthetic implications and the biological activity of chromoazepinone A and B. *Org. Biomol. Chem.*, **8**: 3157-3163.

Momen A.Z.M.R., T. Mizuoka and T. Hoshino, 1998. Studies on the biosynthesis of violacein. Part 9. Green pigments possessing tetraindole and dipyrromethene moieties, chromoviridans, produced by a cell-free extract of *Chromobacterium violaceum* and their biosynthetic origins. *J. Chem. Soc., Perkin Trans. I,* 3087-3092.

Momen A.Z.M.R. and T. Hoshino, 2000. Biosynthesis of violacein: Intact incorporation of the tryptophan molecule on the oxindole ring side, with intramolecular rearrangement of the indole ring on the 5-hydroxyindole side. *Biosci. Biotechnol. Biochem.*, **64**: 539–549.

Nettleton D., T. Doyle, B. Krishnan, T. Matsumoto and J. Clardy, 1985. Isolation and structure of rebeccamycin - a new antitumor antibiotic from *Nocardia aerocoligenes*. *Tetrahedron Lett.*, **26**: 4011-4014.

Omura S., Y. Iwai, A. Hirano, A. Nakagawa, J. Awaya, H. Tsuchiya, Y. Takahashi and R. Masuma, 1977. A new alkaloid AM-2282 of *Streptomyces* origin. Taxonomy, fermentation, isolation and preliminary characterization. *J:Antibiot.* (Tokyo), **30**: 275-282.

Pauer H., C.C.P. Hardoim, F.L. Teixeira, K.R. Miranda, D.D.S. Barbirato, D.P. de Carvalho, L.C.M. Antunes, A.A.D.C. Leitäo, L.A. Lobo and R.M.C.P. Domingues, 2018. Impact of violacein from *Chromobacterium violaceum* on the mammalian gut microbiome. *Plos one*, **13**: e0203748 (Review).

Qu Y., X. Zhang, Q. Ma, F. Ma, Q. Zhang, X. Li, H. Zhou and J. Zhou, 2012. Indigo biosynthesis by *Comamonas* sp. MQ. *Biotechnol. Lett.*, **34**: 353-357.

Rodrigues A.L., N. Trachtmann, J. Becker, A.F. Lohanatha, J. Blotenberg, C.J. Bolten, C. Korneli, A.O. de Souza Lima, L.M.G. Porto, A. Sprenger and C. Wittmann, 2013. Systems metabolic engineering of *Escherichia coli* for production of the antitumor drugs violacein and

deoxyviolacein. *Metab Eng*, **20**: 29-41 (Review).

Ryan K.S., C.J. Balibar, K.E. Turo, C.T. Walsh and C.L. Drennan, 2008. The violacein biosynthetic enzyme VioE shares a fold with lipoprotein transporter proteins. *J. Biol. Chem.*, **283**: 6467-6475.

Ryan K.S. and C.L. Drennan 2009. Divergent pathways in the biosynthesis of bisindole natural products. *Chem. Biol.* 16: 351-364 (Review).

Sánchez C., A.F. Braña, C. Mendez and J.A. Salas, 2006. Reevaluation of the violacein biosynthetic pathway and its relationship to indolocarbazole biosynthesis. *ChemBioChem*, **7**: 1231-1240.

Shinoda K., T. Hasegawa, H. Sato, M.Shinozaki, H. Kuramoto, Y. Takamiya, T.Sato, N. Nikaidou, T. Watanabe and T. Hoshino, 2007. Biosynthesis of violacein: a genuine intermediate, protoviolaceinic acid, produced by VioABDE, and insight into VioC function. *Chem. Commun.*, 4140-4142.

Timmusk T., M. Lopp, E.Vasar, A. Kaasik and M. Karelson, 2017. Preparation of indolylmethylene oxindoles as TRK receptor antagonists. *U.S. Pat. Appl. Publ.*, US 20170057948 A1 20170302.

Chromobacteriumu violaceum のブロック変異株 B-4で生産されるビスインドール系化合物インデルビンと indol-3-ylmethylene-2-oxoindole およびこれらの推定生合成経路

田村博康[1,2]・佐藤正人[1,2]・樋熊　学[2]・坂口良子[2]・佐々木勇輔[2]・星野　力[1,2]*

（2020年10月７日受付）

要　約

細菌 *Chromobacterium violaceum* は青紫の色素ビオラセインを生産する。我々の研究室では、長年生合成経路の解明に携わってきた。その過程で、新規なインドール系アルカロイド化合物を発見し報告してきた。本報告では、全くビオラセイン色素を生産しないブロック変異株 B-4を得て、そのトリプトファン代謝産物を調べた。B-4が生産する赤色**16**や黄色色素**17**を精製・単離し、主に各種二次元 NMR（^{1}H-^{1}H COSY, NOESY, HSQC, HMBC）を用いてそれらの構造を解明した。インデルビン**16**及び(*Z*)-indol-3-ylmethylene-2-oxoindole **17**と判明した。*C. violaceum* による両者の代謝物の生産の報告例はなくはじめての例である。生合成経路を推定した。また、ビオラセインは5つの ORF VioA, B, C, D, E 及び非酵素的な酸素添加過程の関与から成り立っているが、indol-3-ylmethylene-2-oxoindole 17の生成は、*vio*A, B, D, E 遺伝子が破壊されたが、フラビン補酵素をもつ *vio*C 遺伝子が酸素添加酵素としての機能を有していた結果として生産されたと推定した。

新大農研報, 73:1-11, 2021

キーワード：ビオラセイン、ビスインドール、インデルビン、(*Z*)-indol-3-ylmethylene-2-oxoindole、*Chromobacterium violaceum*

[1] 新潟大学大学院自然科学研究科

[2] 新潟大学農学部

* 代表者：hoshitsu@emeritus.niigata-u.ac.jp